

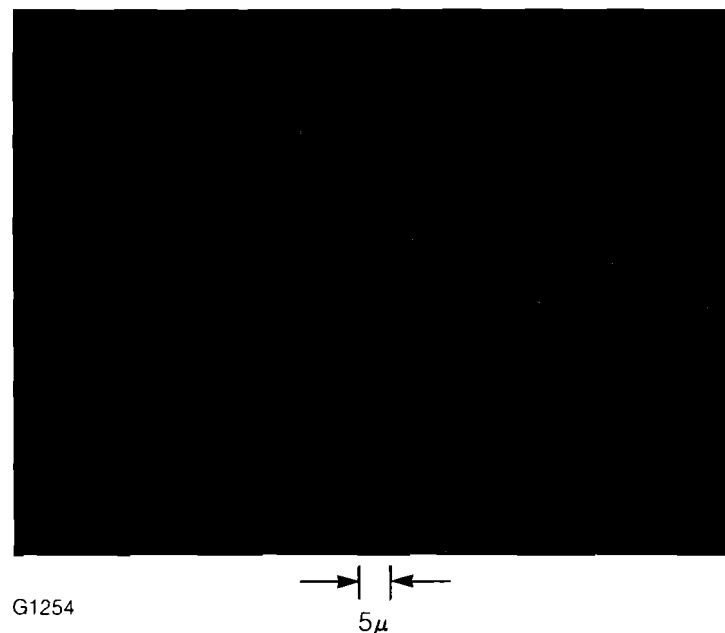
### 3.B Defects and Damage in Thin Films

As the laser-fusion community proceeds to frequency-convert Nd:glass laser systems to shorter wavelengths, the importance of the performance of optical coatings at these wavelengths becomes of greater interest. Of particular interest to the LLE program is the performance of these coatings at the tripled frequency of Nd:glass, 351 nm. The fluence level at which the optical coatings can transport the UV beam will have a major impact on the size, cost, and energy-on-target of all UV upgrades to the OMEGA laser. We have therefore developed an experimental system to characterize better the damage process in thin-film coatings.

Presently the most successful theory<sup>1,2</sup> describing the damage of optical thin films by high-power laser radiation attributes the damage process to isolated microscopic impurities, or defects, in the deposited coating. According to this theory, the impurity absorbs the incident radiation causing its temperature to rise, eventually producing melting, vaporization, or fracture of the material surrounding the impurity.

This impurity model can explain many of the scaling effects observed in thin-film damage studies. The observed decrease in damage threshold with decreasing wavelength can be attributed to the increase in Mie absorption with decreasing particle size, and the well-known result that Mie scattering is strongest for particles whose size is comparable to the incident light wavelength. The observation that the damage threshold increases with thinner films can be explained by the exclusion of larger, easier-to-damage, impurities as the physical thickness of the film is reduced. The observation of very high damage thresholds for small incident-laser spot sizes is consistent with damage being caused by localized impurities: when the spot size is small

Fig. 23  
Photomicrograph of typical damage to a  $Ta_2O_5$ - $SiO_2$  high-reflectance (HR) coating. Note in particular the micron-sized pits.



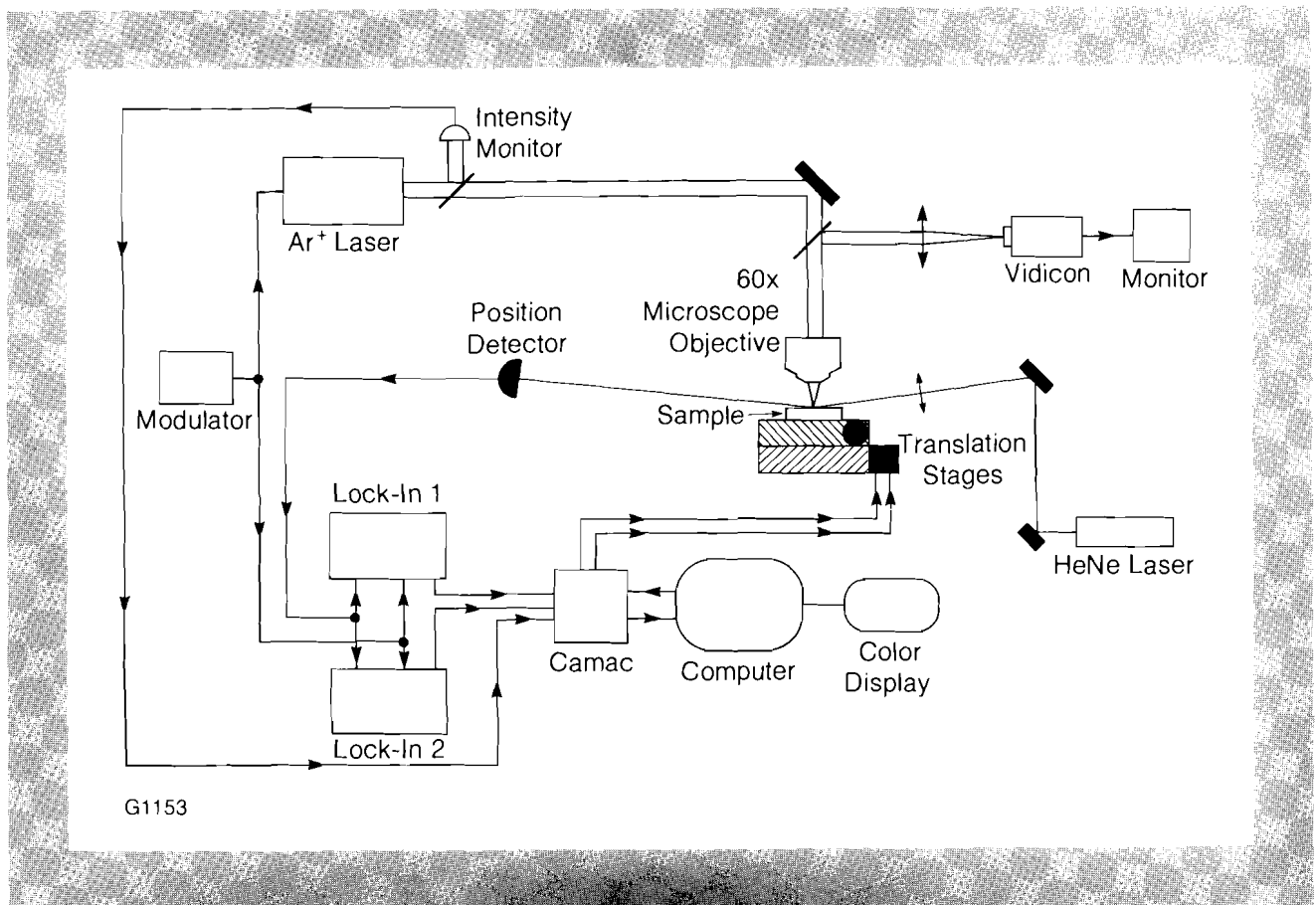
compared with the mean distance between impurities, it is possible to avoid these weaker areas and measure higher thresholds. In addition, it has been shown for oxide and fluoride films that the dependence of damage and thermal properties on laser pulse width is consistent with the impurity model.<sup>1</sup>

Very little, however, is known about the exact nature or density of these damage-causing impurities. It has been determined from damage morphology<sup>3-5</sup> that the impurities must be small in size, typically several microns or less in diameter. Figure 23 shows a photomicrograph of the typical morphology seen as a result of laser-induced damage. In this work we have set out to establish a direct connection between the localized absorption properties of a thin film and the appearance of damage in areas of locally high absorption.

### Detection of Impurities

Several attempts have been made to use photothermal effects to investigate surface and subsurface structure in solids and in thin films.<sup>6-11</sup> Photothermal imaging has developed into a very powerful non-destructive testing technique. All previous methods have lacked sufficient spatial resolution to detect the objects of interest to laser-damage studies, of size  $\leq 1 \mu\text{m}$ . Some defects have been seen in thin films,<sup>7-10</sup> but their size, typically 20 microns

Fig. 24  
Block diagram of the "Mirage" apparatus for photothermal deflection.



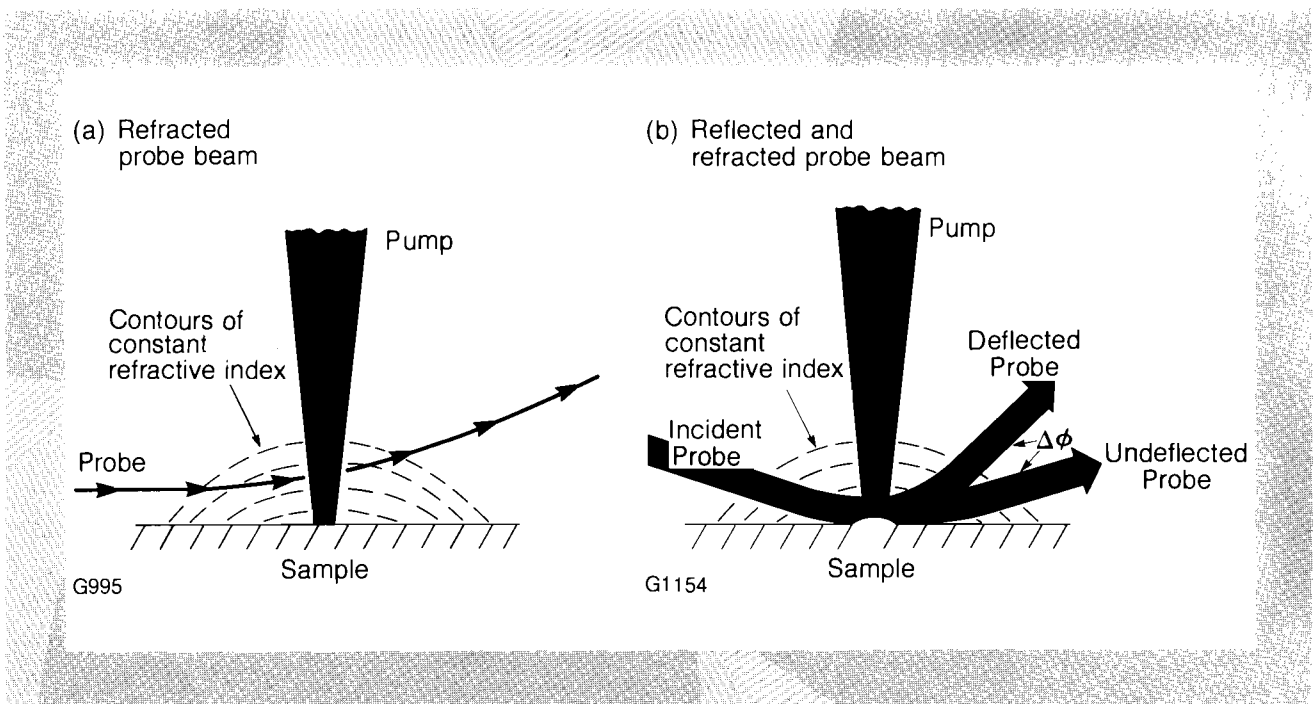
or larger, is not consistent with the experimental observation of micron-size pits in damage coatings at threshold (see Fig. 23).

The apparatus we have used to locate micron-size absorbing impurities in dielectric thin films is shown schematically in Fig. 24. It relies on the photothermal deflection<sup>11</sup> of a probe laser to measure the absorption, in a localized area, of energy from the pump laser. The pump beam consists of modulated 0.351- $\mu\text{m}$  light from an argon-ion laser focused to a  $1.0 \pm 0.2\text{-}\mu\text{m}$ -diameter spot by a 60 $\times$  microscope objective. The sample of interest is kinematically mounted on a computer-controlled X-Y translation stage, with a minimum step size of 0.4  $\mu\text{m}$ . A HeNe laser probe beam has been used in two geometries: skimming across the sample (Fig. 25a), and reflecting off the sample surface at a shallow angle (Fig. 25b).<sup>10</sup> The probe beam is focused to a spot size of 75  $\mu\text{m}$  in the vicinity of the pump-beam focus. The two probe-beam geometries have been compared and the second (reflective) method has shown a sensitivity greater by a factor of ten. This can most probably be attributed to a new photothermal effect first discussed by Olmstead *et al.*<sup>12</sup>

Fig. 25

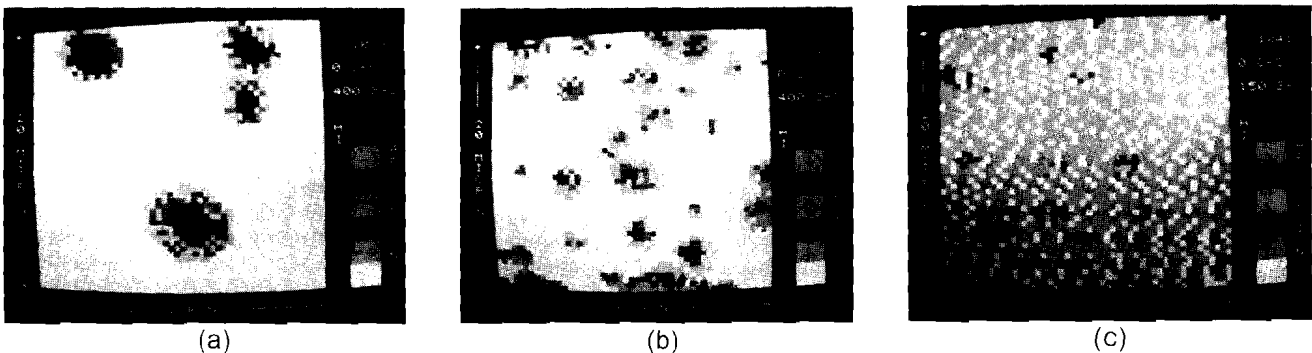
Use of the "Mirage" effect for mapping defects in a thin-film sample. Pump-laser energy is absorbed by a defect with two consequences: (1) the surrounding air is heated, leading to a refractive-index gradient; and (2) thermal expansion in the absorption region causes a "bump" to form on the sample surface. Depending on the geometry chosen, the probe laser is either refracted [case (a)] or reflected as well as refracted [case (b)].

In the skimming geometry (Fig. 25a), the probe beam is deflected by a refractive-index gradient, caused by the temperature gradient set up when the pump beam is absorbed locally by an impurity in the sample. This effect is also present in the reflective geometry (Fig. 25b), but here the probe beam is also deflected off the "bump" caused by the local heating and resulting thermal expansion of the substrate. The modulated position of the probe laser is measured by a position sensor (United Detector Technologies SC-25) connected to a set of lock-in amplifiers arranged in quadrature to measure both the amplitude and phase



of the position signal. A DEC-11 / 23 computer controls the position of the sample and reads the output of the lock-in amplifiers. False-color absorption maps of the coatings being studied are produced on a Chromatics color-graphics display. The spatial resolution obtainable using this technique is illustrated in Fig. 26, where scans of absorbing sites of Cr spots of various diameters ( $\leq 5 \mu\text{m}$ ,  $\leq 1 \mu\text{m}$ , and  $\leq 0.4 \mu\text{m}$ ) are shown. The  $0.4\text{-}\mu\text{m}$  sites are clearly resolvable.

When the cross section of the absorbing volume becomes smaller than the diameter of the pump beam, only a portion of the incident energy is transformed into heat and into the resulting thermal and acoustic waves. The ultimate detectivity in this case will depend not only on the absorption coefficient and the thickness of the inclusion, but also on the ratio of the cross sections of the pump beam and the absorbing region, the distance between the inclusion and the coating-substrate interface, and the thermal properties of the material in which the inclusion is embedded. It should be clear that the pump-beam spot size must be kept as small as possible in order to detect the absorbing inclusions in thin films with maximum sensitivity.



G1253

Fig. 26

Absorption maps of Cr impurity particles of various diameters ( $d$ ).

(a)  $d \leq 5 \mu\text{m}$

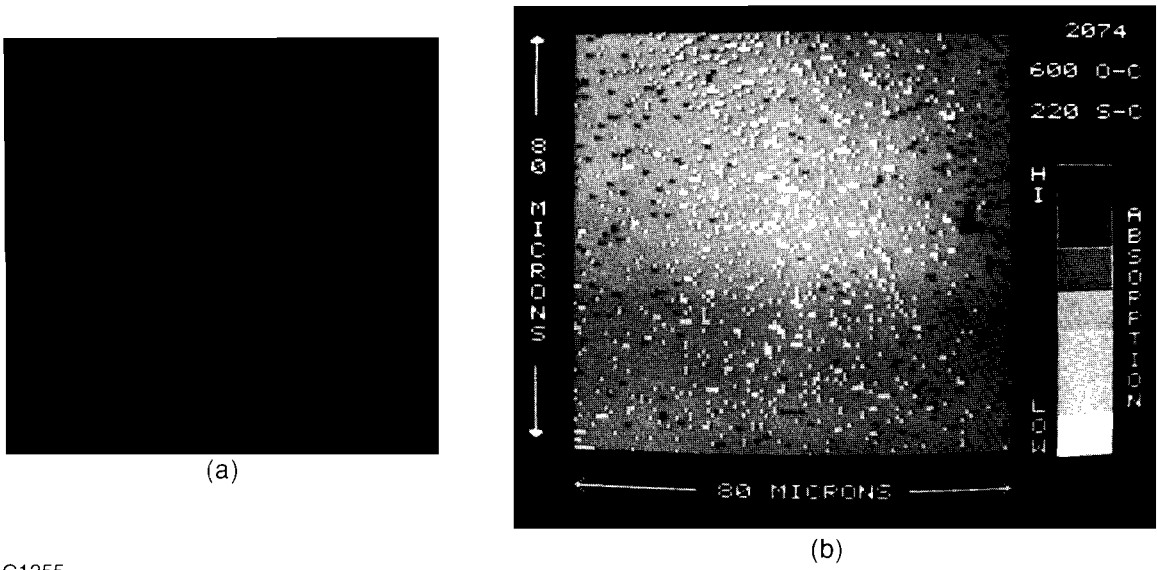
(b)  $d \leq 1 \mu\text{m}$

(c)  $d \leq 0.4 \mu\text{m}$

### Impurities and Damage

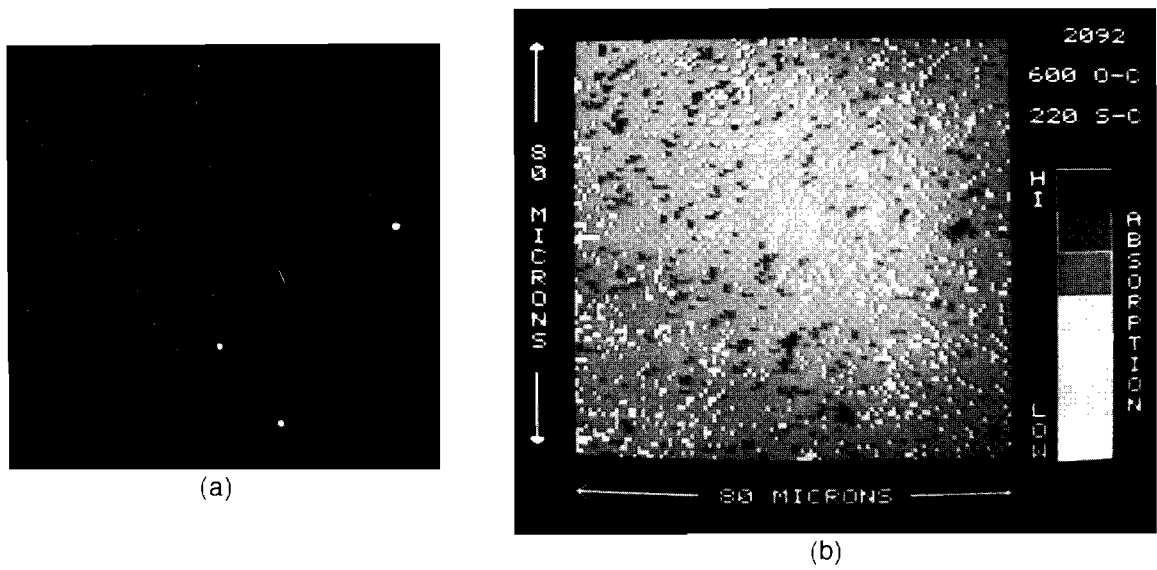
In order to demonstrate a connection between absorptive impurities and damage, we have made absorption maps of several coatings and then exposed them to high-intensity laser light on the LLE UV damage-testing facility.<sup>13</sup> Photomicrographs and absorption maps of sample coatings were taken both before and after the damage test. Typical examples are shown in Figs. 27 and 28. In many cases the absorption map before damage shows small areas of high absorption that are not visible in the dark-field photomicrographs (see Fig. 27). When the coating shown in Fig. 27 was exposed to a laser irradiance approximately 20% above its damage threshold, three localized areas on the coating were damaged as is seen in the photomicrograph of Fig. 28a.

In addition, the absorption map of the same area (Fig. 28b) shows clearly increased absorption in the region which showed a defect in Fig. 27b. There are also two areas which show damage in Fig. 28b but no strong absorption signature in Fig. 27b. In these cases, it is uncertain whether our sensitivity is insufficient to



G1255

Fig. 27  
(a) Photomicrograph and (b) absorption map of Ta<sub>2</sub>O<sub>5</sub>-SiO<sub>2</sub> HR coating before damage test.



G1256

Fig. 28  
(a) Photomicrograph and (b) absorption map of Ta<sub>2</sub>O<sub>5</sub>-SiO<sub>2</sub> HR coating after damage test.

detect the damage-causing impurities, or whether other mechanisms besides linear absorption are acting to initiate some of the damage. Attempts are being made to increase the sensitivity of our apparatus in order to explore this question further.

## Conclusion

We have taken a first step toward understanding the role of absorptive inclusions in the damage process of thin films. We have demonstrated that photothermal-deflection microscopy can detect submicron absorbing impurities in optical coatings. In the future, we plan to identify the exact nature of these damage-causing impurities. It is hoped that optical coatings of increased damage resistance will be obtained by the use of measures to control these impurities in the manufacturing process.

## REFERENCES

1. T. W. Walker, A. H. Guenther, and P. E. Nielsen, *IEEE J. Quantum Electron.* **17**, 2053 (1981).
2. See references 21-48 in Ref. 1.
3. W. H. Lowdermilk, D. Milam, and F. Rainer, in "*Laser-Induced Damage in Optical Materials*," edited by H. E. Bennett, A. J. Glass, A. H. Guenther, and B. E. Newnam, NBS Special Publ. 568, 391, Washington, D.C., GPO (1979).
4. C. K. Carniglia, J. H. Apfel, T. H. Allen, T. A. Tyttle, W. H. Lowdermilk, D. Milam, and F. Rainer, in "*Laser-Induced Damage in Optical Materials*," edited by H. E. Bennett, A. J. Glass, A. H. Guenther, and B. E. Newnam, NBS Special Publ. 568, 377, Washington, D.C., GPO (1979).
5. T. W. Walker, A. H. Guenther, and P. E. Nielsen, *IEEE J. Quantum Electron.* **17**, 2041 (1981).
6. Y. H. Wong, R. L. Thomas, and G. F. Hawkins, *Appl. Phys. Lett.* **32**, 538 (1978).
7. R. P. Freese and K. J. Teegarden, in "*Laser-Induced Damage in Optical Materials*," edited by H. E. Bennett, A. J. Glass, A. H. Guenther, and B. E. Newnam, NBS Special Publ. 568, 313, Washington, D.C., GPO (1979).
8. D. S. Atlas, M. S. Thesis, Institute of Optics, University of Rochester, 1981.
9. J. A. Abate, S. D. Jacobs, W. S. Piskorowski, and T. P. Pottenger, *Proceedings of the Second Conference on Lasers and Electro-Optics (CLEO)*, Phoenix, AZ (1982).
10. W. C. Mundy, R. S. Hughes, and C. K. Carniglia in "*Laser-Induced Damage in Optical Materials*," edited by H. E. Bennett, A. H. Guenther, D. Milam, and B. Newnam, NBS Special Publication, 1982 (to be published).
11. A. C. Boccara, D. Fournier, and J. Badoz, *Appl. Phys. Lett.* **36**, 130 (1980).
12. M. Olmstead, N. M. Amer, D. Fournier, and A. C. Boccara, *Appl. Phys.* (to be published).
13. J. A. Abate, R. Roides, S. D. Jacobs, W. Piskorowski, and T. Chipp in "*Laser-Induced Damage in Optical Materials*," NBS Special Publication, 1982 (to be published).